Conditional Servo-compensator of an Airlaunch System

Cuong Nguyen Van, Gilney Damm

Conditional Servo-compensator of an Airlaunch System*

Van Cuong Nguyen and Gilney Damm

Abstract— **A Multiple Input Multiple Output (MIMO) controller based on the conditional servo-compensator technique is designed for the robust stabilization of a new satellite launching strategy called (unmanned) airlaunch. This strategy consists in using a two-stages launching system. The first stage is composed of an airplane (manned or unmanned) that carries a rocket launcher which constitute the subsequent stages. The control objective is to stabilize the aircraft in the launch phase. It is developed separately for two nonlinear motion modes of the model, the longitudinal and lateral modes, and is applied to the full multi-input multi-output model of the aircraft. The controller is indeed able to assure system stability for rather large disturbances. Performance of the proposed control algorithm is illustrated through simulations.**

I. Introduction

This work presents the design of a controller for the robust stabilization of a new satellite launching strategy called (unmanned) airlaunch. This strategy consists in using a two-stages launching system. The first stage is composed of an airplane that carries a rocket launcher which constitutes the subsequent stage. The aircraft brings the rocket to a desired drop area, consequently avoiding many costs and risks related to land rocket launching. On the other hand, this procedure brings up many other difficulties connected to the instant of releasing the rocket.

Currently, several airlaunch systems are under development (see [14], [3]). Most current airlaunch projects use standard or lightly modified airplanes as first stage. For example, there has been tests using F15, C17, B52, L-1011 in Rascal, QuickReach, Proteus and Pegasus projects. Unlike those, other projects aim to develop an airlaunch system that uses an unmanned aerial vehicle (UAV) instead of a standard aircraft with a human pilot inboard. The objective is then to use an UAV to fly the launcher to the desired drop point. There are many advantages in doing so, in first place safety since no human lives are involved during the delicate launching phase. In addition, since there is no need for life supporting devices, weight is restricted to the strict minimum. Finally, mission may take as long as necessary without human restrictions as tiredness.

The present paper addresses the stabilization of the drop phase. It intends to introduce a robust control scheme for this complex procedure. In fact, airlaunch may be very delicate for many reasons. For example, since the rocket may be almost as heavy as the UAV, this means that the aircraft will instantaneously lose almost half of its mass. Current airlaunch systems present a much smaller ratio launcher/aircraft and rely on human pilot to stabilize the aircraft during and immediately after the launching instant. The proposed system must replace the human pilot in this stabilization task, with a much more adverse mass ratio. In the same way, the two-stages system is strongly nonlinear and can even for small perturbations be brought quite far from the initial equilibrium point. Furthermore, available models are based on experiments for different flight conditions, with lookup tables and polynomial interpolation between these points. For this reason, parameters and even models are not very well known, and need very robust control schemes like those found in [5].

Our previous works proposed a new strategy based on MIMO conditional integrator (see [2]) for the nonlinear model to stabilize the airlaunch system after the launching phase, which is modeled by the Initial conditions aproach [12] and by Perturbation on aerodynamic force and moment in [11]. The designed controller resulted in a better behavior in these extreme situation that are nevertheless expected in the unmanned airlaunch. This paper is an extension of the previous works using the MIMO Conditional Servocompensator based controller developed in a series of papers ([7], [4] and [1]) to stabilize the airlaunch system in the case where the launching phase is modeled by perturbation on aerodynamic force and moment (see [11]).

The paper is organized as follows: in section II, we describe the nonlinear mathematical system model based on [13],[16] and [10]. The control design literature is discussed in section III, and its application to the full nonlinear system model in section IV. The paper is completed by some computer simulations and conclusions.

II. Modeling

Drop phase is delicate to model, and requires a large amount of data and previous knowledge about the real system. It can also be represented as a hybrid system composed by two (or three) continuous models that are switched. These models represents the system before, (possible during) and after the separation phase. In the present work we have adopted this strategy, we have considered three phases, using two aircraft models.

1) before the separation $\Rightarrow$ The first aircraft model (representing the UAV and the rocket) is in an stable operating condition
2) during the separation $\Rightarrow$ a second aircraft model representing only the UAV, starting on the previous

*The research leading to these results has received funding from the European Union Seventh Framework Programme [FP7/2007-2013] under grant agreement n257462 HYCON2 Network of excellence

Van Cuong Nguyen is with IBISC - Université d'Evry Val d'Essonne, Evry, France vancuong.nguyen@ibisc.fr

Gilney Damm is with IBISC - Université d'Evry Val d'Essonne, Evry, France gilney.damm@ibisc.fr

operating condition is disturbed by impulses on forces and moments. These disturbances are inside a time interval T_{int} and represent a not perfect separation. Furthermore the initial conditions, inherited from the first phase, are not an equilibrium point for the second aircraft model.

3) after the separation $\Rightarrow$ the disturbances stop (UAV and rocket are not in physical contact anymore). It can be shown that the effect of launching the rocket from the UAV impacts most the lift force, and the roll and pitch moments. We suppose that these perturbing force and moments are constant during interval T_{int}, and we represent then F_{z_p}, L_p and M_p for the perturbations on the lift force, on the roll moment and pitch moment respectively. In the present work we will study a worst case of disturbance. We consider that the separation phase is not simultaneous in all links that attach the rocket and the UAV. For this reason, the rocket remains attached to one end of the UAV during T_{int}. We have then studied how long the disturbance could last and that the control algorithm could still stabilize the aircraft back.

We have then assumed that:

- the perturbation on lift force during T_{int} is equal the rocket's mass times gravity, that means $F_{z_p} = mg$.
- the perturbation on pitch moment during T_{int} is $M_p = mgl_r/2$ where l_r is the rocket length.
- the perturbation on roll moment during T_{int} is small, because of the geometry of the rocket (thin and long).
- the model following the launch phase is that of an F-16. Its initial condition is the equilibrium point of the model previous the launch phase. This is taken as the F-16 model with twice the F-16's mass.

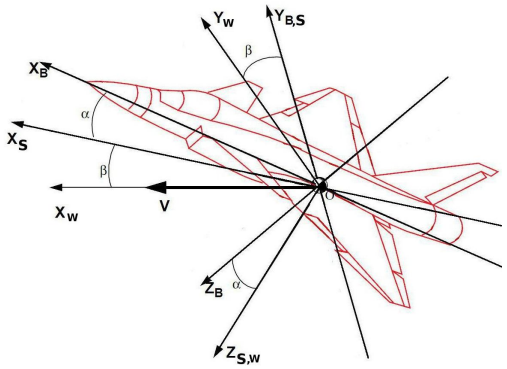

Fig. 1. Frames: Body fixed axes $OX_BY_BZ_B$, Stability axes $OX_SY_SZ_S$, Aerodynamic axes $OX_WY_WZ_W$

Following this procedure, the F-16 aircraft in the instant following the dynamic airlaunch is described in the aerodynamic axes (the aerodynamic axes $OX_WY_WZ_W$ in the Fig. 1) i.e. the reference frame attached to the airspeed vector (V). The system dynamics can be expressed as (see [16] and [17]):

In (1), $I_{xx}, I_{yy}, I_{zz}, I_{xz}$ are the moments of inertia, m is the mass of the system (kg) and g the gravity constant. $\alpha, \beta, V, p, q, r, \phi, \theta, \psi$ are the state variables of the airlaunch aircraft model, they are the angle of attack, sideslip, airspeed, roll rate, pitch rate, yaw rate, roll angle, pitch angle and yaw angle respectively. $\alpha, \beta, \phi, \theta, \psi$ are expressed in rad, p, q, r in rad/s and V in m/s. T is the thrust force, F_x, F_y, F_z and L, M, N are aerodynamic forces and moments respectively. All forces and moments are expressed in N and Nm.

$$
\begin{cases}
\dot{\alpha} = -\cos\alpha\tan\beta p + q - \sin\alpha\tan\beta r \\
-\frac{\sin\alpha}{mV\cos\beta}(T + F_x) + \frac{\cos\alpha}{mV\cos\beta}F_z \\
+\frac{g}{V\cos\beta}[\sin\alpha\cos\theta + \cos\alpha\cos\phi\cos\theta] \\
\dot{\beta} = \sin\alpha p - \cos\alpha r - \frac{\cos\alpha\sin\beta}{mV}[T + F_x] + \frac{\cos\beta}{mV}F_y \\
-\frac{\sin\alpha\sin\beta}{mV}F_z + \frac{g}{V}[\cos\alpha\sin\beta\sin\theta \\
+\cos\beta\cos\theta\sin\phi - \sin\alpha\sin\beta\cos\phi\cos\theta] \\
\dot{V} = \frac{\cos\alpha\cos\beta}{m}[T + F_x] + \frac{\sin\beta}{m}F_y \\
+\frac{\sin\alpha\cos\beta}{m}F_z + g[\cos\alpha\cos\beta\sin\theta \\
+\sin\beta\sin\phi\cos\theta + \sin\alpha\cos\beta\cos\phi\cos\theta] \\
\dot{p} = \frac{1}{I_{xx}I_{zz} - I_{xz}^2}[(I_{yy}I_{zz} - I_{zz}^2 - I_{xz}^2)rq - I_{xz}(I_{xx} \\
+I_{zz} - I_{yy})pq + I_{zz}L - I_{xz}N] \\
\dot{q} = \frac{1}{I_{yy}}[(I_{zz} - I_{xx})pr + I_{xz}(p^2 - r^2) + M] \\
\dot{r} = \frac{1}{I_{xx}I_{zz} - I_{xz}^2}[(-I_{xx}I_{yy} + I_{zz}^2 + I_{xz}^2)pq \\
+I_{xz}(I_{xx} + I_{zz} - I_{yy})rq + I_{xx}N - I_{xz}L] \\
\dot{\phi} = p + \tan\theta(q\sin\phi + r\cos\phi) \\
\dot{\theta} = q\cos\phi - r\sin\phi \\
\dot{\psi} = \frac{q\sin\phi + r\cos\phi}{\cos\theta}
\end{cases}
\tag{1}
$$

These aerodynamic forces and moments are function of all the considered states. In this model, these aerodynamic forces and moments are under look-up table from wind tunnel data measurements as may be found in [10]. Finally, the control inputs are respectively the aileron (δ_a), rudder (δ_r) and elevator (δ_e) angles.

This model is based on wind tunnel data from NASA, considering the following conditions:

- angle of attack is in the range of $[-10°, 45°]$ and sideslip of $[-30°, 30°]$
- flag deflection is ignored
- physical constraints for aileron ($|\delta_a| \leq 21.5°$), rudders ($|\delta_e| \leq 25°$) and elevator ($|\delta_r| \leq 30°$)
- all actuators are modeled as a first order model ($\tau = 1/0.0495s$) with limit rates $60°/s$ for aileron and elevator, and $120°/s$ for rudder.

In particular, we use the low quality mode of the F-16 model, and the aerodynamic data is interpolated and extrapolated linearly in simulation from tables found in [10].

III. Control design

A. Conditional servo-compensator control design

The MIMO conditional servo-compensator controller design for the output regulation of a class of minimum-phase nonlinear systems in case of asymptotically constant references is studied in [7], [4] and [2]. These papers concern a servo-compensator performing as a sliding mode controller outside the boundary layer, and performing as a conditional one that provides servo-compensation only inside the boundary layer. First results have studied the SISO case with a scalar sliding surface and the asymptotic stability of the system inside a boundary layer. These results were

extended in [15] and [8] for linearized MIMO systems under some additional assumptions. Our present work is dedicated to use a nonlinear extension of these results developed in [1], for stabilizing an unmanned aircraft after the airlaunch phase.

Consider the system:

$$\begin{cases} \dot{e}_1 &= e_2 \\ \dot{e}_2 &= f(e_1,e_2)+g(e_1,e_2)u \end{cases} \quad (2)$$

where $e_1(t) \in \mathbb{R}^n$ is an output error vector, $e_2 = \dot{e}_1$, $u \in \mathbb{R}^n$ control input and $f(e_1,e_2) \in \mathbb{R}^n$, $g(e_1,e_2) \in \mathbb{R}^{n\times n}$ are continuous functions.

Let us define the sliding surface as:

$$s = K_0\sigma + K_1 e_1 + e_2 \quad (3)$$

where $\sigma \in \mathbb{R}^n$ is the output of the conditional servo-compensator

$$\dot{\sigma} = -K_0\sigma + \mu sat(s/\mu) \quad (4)$$

in which μ is the boundary layer, K_0 is a positive definite matrix, $K_1 \in \mathbb{R}^{n\times n}$ is chosen such a way that $K_1 + sI_n$ is Hurwitz.

The saturation function is determined as:

$$sat(s/\mu) = \begin{cases} s/\|s\| & \text{if } \|s\| \geq \mu \\ s/\mu & \text{if } \|s\| < \mu \end{cases} \quad (5)$$

The previous work [2] has shown that system (2) is exponentially stabilized by the controller called Conditional Integrator in the case where K_0 is a scalar. The paper [1] extends the result for the case of K_0 being a matrix. The controller is called Conditional Servo-compensator controller that we remind as below.

We denote $\mathcal{O}_\mu$ as the region neighborhood of $(e_1,e_2) = (0,0)$ with a radius R_μ for $\|s\| < \mu$

$$\mathcal{O}_\mu = \{e=(e_1,e_2) \in \mathbb{R}^n \times \mathbb{R}^n \mid \|e\| \leq R_\mu\} \quad (6)$$

We state the following assumptions on the forcing terms $f(e_1,e_2)$ and $g(e_1,e_2)$ to design the control algorithm.

Assumption 3.1: $f(e_1,e_2)$ is bounded by a function of $\gamma(\|e_1\| + \|e_2\|)$ (where $\gamma(\cdot)$ is a class $\mathcal{K}$ function) and a positive constant Δ_0 :

$$\|f(e_1,e_2)\| \leq \gamma(\|e_1\| + \|e_2\|) + \Delta_0$$

and as a consequence,

$$\|f(e_1=0,e_2=0)\| = \|f(0,0)\| \leq \Delta_0$$

for $(e_1,e_2) \in \mathbb{R}^n \times \mathbb{R}^n$. Inside the boundary layer, the function $f(e_1,e_2)$ is required to be Lipschitz for $(e_1,e_2) \in \mathcal{O}_\mu$, as a consequence

$$\|f(e_1,e_2) - f(0,0)\| \leq L_1\|e_1\| + L_2\|e_2\|$$

$\gamma(\|e_1\|+\|e_2\|)$ is also required to be Lipschitz for $(e_1,e_2) \in \mathcal{O}_\mu$:

$$\gamma(\|e_1\| + \|e_2\|) \leq \gamma_1\|e_1\| + \gamma_2\|e_2\|$$

Assumption 3.2: Function $g(e_1,e_2)$ is continuous and invertible for all $(e_1,e_2) \in \mathbb{R}^n \times \mathbb{R}^n$.

Following these conditions, the controller u defined below can be applied to (2) to stabilize the system:

$$\begin{cases} u = -\Pi(e_1,e_2)\text{sat}(s/\mu) \\ \Pi(\cdot) = g^{-1}(\cdot)(\Pi_0 + \mu K_0 + (\gamma(\cdot)+\Delta_0)I_n) \end{cases} \quad (7)$$

Π_0 is a positive definite matrix, μ is the boundary layer and K_0 is a positive definite matrix as defined above.

The stability of the control law (7) for system (2) can be demonstrated following the results of [1].

B. Longitudinal control design

In the longitudinal control design, we assume that all lateral state variables are null or constant, only longitudinal states are time varying. Moreover it is assumed that the airspeed's response is much slower than other states, and that the control surface deflection has no effects on the aerodynamic force components (lift and drag) but only on moments.

Aerodynamic forces F_x, F_z and moment M can be calculated by its aerodynamic coefficients (see more in [6]). $F_x = (C_x(\alpha) + \bar{c}C_{x_q}(\alpha)q/(2V))\bar{q}S$, $F_z = (C_z(\alpha,\beta) + \bar{c}C_{z_q}(\alpha)q/(2V))\bar{q}S$, $M = (C_m(\alpha) + C_{m_q}(\alpha)q\bar{c}/(2V) + C_{m_{\delta_e}}(\alpha)\delta_e)\bar{q}S\bar{c}$. By replacing F_x, F_z, moment M and $\beta = 0$, $\phi = 0$, $p = 0$, $r = 0$ in (1). The model for longitudinal dynamic can be written as:

$$\begin{cases} \dot{\alpha} = \frac{1}{mV}[-\sin\alpha(T + C_x(\alpha)\bar{q}S) + \cos\alpha C_z(\alpha)\bar{q}S] \\ \quad +q + \frac{\rho S}{4m}(-\sin\alpha C_{x_q}(\alpha)\bar{c} + \cos\alpha C_{z_q}(\alpha)\bar{c})q \\ \quad + \frac{g}{V}\cos(\theta_0 - \alpha) \\ \dot{q} = I_7\bar{q}S(C_m(\alpha)\bar{c} + C_{m_q}(\alpha)\bar{c}q + C_{m_{\delta_e}}(\alpha)\bar{c}\delta_e) \\ \dot{\theta} = q \end{cases} \quad (8)$$

in which S is wing area, $\bar{q}$ air pressure, $\bar{c}$ equivalent width, $I_7 = 1/I_{yy}$, $C_x(\alpha)$, $C_{x_q}(\alpha)$, $C_z(\alpha)$, $C_{z_q}(\alpha)$, $C_m(\alpha)$, $C_{m_q}(\alpha)$ $C_{m_{\delta_e}}(\alpha)$ are aerodynamic coefficients taken from [9].

Equation (8) can be rearranged as:

$$\begin{cases} \dot{\theta} &= q \\ \dot{\alpha} &= f_{11}^\alpha(\alpha) + (1 + f_{12}^\alpha(\alpha))q + f_{13}^\alpha(\alpha,\theta) \\ \dot{q} &= f_{21}^\alpha(\alpha) + f_{22}^\alpha(\alpha)q + g_2^\alpha(\alpha)\delta_e \end{cases} \quad (9)$$

where $f_{11}^\alpha(\alpha)$, $f_{12}^\alpha(\alpha)$, $f_{13}^\alpha(\alpha,\theta)$, $f_{21}^\alpha(\alpha)$, $f_{22}^\alpha(\alpha)$ and $g_2^\alpha(\alpha)$ represent the terms of (8) respectively.

Let us define $x_1^\alpha = \alpha$, $x_2^\alpha = \dot{x}_1^\alpha = \dot{\alpha}$ and $u^\alpha = \delta_e$, which allow us to rewrite (9) into:

$$\dot{\theta} = \eta^\alpha(x_1^\alpha, x_2^\alpha, \theta) \quad (10a)$$

$$\dot{x}_1^\alpha = x_2^\alpha$$

$$\dot{x}_2^\alpha = F^{\alpha\prime}(x_1^\alpha, x_2^\alpha, \theta) + G^{\alpha\prime}(x_1^\alpha, x_2^\alpha)u^\alpha \quad (10b)$$

where

$$\begin{cases} \eta^\alpha(\cdot) = (x_2^\alpha - f_{11}^\alpha(x_1^\alpha) - f_{13}^\alpha(x_1^\alpha,\theta))/(1 + f_{12}^\alpha(x_1^\alpha)) \\ F^{\alpha'}(\cdot) = \frac{\partial f_{11}^\alpha(x_1^\alpha)}{\partial x_1^\alpha}x_2^\alpha + \frac{\partial f_{13}^\alpha(x_1^\alpha)}{\partial x_1^\alpha}x_2^\alpha \\ \qquad +(1 + f_{12}^\alpha(x_1^\alpha))f_{21}^\alpha(x_1^\alpha) + (\frac{\partial(1+f_{12}^\alpha(x_1^\alpha))}{\partial x_1^\alpha}x_2^\alpha \\ \qquad +(1 + f_{12}^\alpha(x_1^\alpha))f_{22}^\alpha(x_1^\alpha))\frac{(x_2^\alpha - f_{11}^\alpha(x_1^\alpha) - f_{13}^\alpha(x_1^\alpha))}{(1+f_{12}^\alpha(x_1^\alpha))} \\ G^{\alpha'}(\cdot) = (1 + f_{12}^\alpha(x_1^\alpha))g_2^\alpha(x_1^\alpha) \end{cases} \quad (11)$$

We define now the reference for the angle of attack α_{ref} considered as constant in this study, and the error vector of angle of attack $e_1^\alpha = x_1^\alpha - x_{1ref}^\alpha = \alpha - \alpha_{ref}$ and the variable $e_2^\alpha = \dot{e}_1^\alpha$. Equation (10b) can be transformed into (12):

$$\begin{cases} \dot{e}_1^\alpha &= e_2^\alpha \\ \dot{e}_2^\alpha &= F^\alpha(e_1^\alpha, e_2^\alpha, \theta) + G^\alpha(e_1^\alpha, e_2^\alpha)u^\alpha \end{cases} \tag{12}$$

Here we remark that $G^\alpha(x_1^\alpha, x_2^\alpha)$ is invertible, and that $F^\alpha(x_1^\alpha, x_2^\alpha, \theta)$ and $G^\alpha(x_1^\alpha, x_2^\alpha)$ are Lipschitz for the entire domain of actuation of the system.

Applying the control algorithm presented in (7) for system (12) (in this case a nonlinear single input single output system) gives the controller:

$$\begin{cases} u^\alpha = -\Pi^\alpha(\cdot)\text{sat}(s^\alpha/\mu^\alpha) \\ \Pi^\alpha(\cdot) = (G^\alpha)^{-1}(\cdot)(\Pi_0^\alpha + \mu^\alpha K_0^\alpha + \gamma^\alpha(\cdot) + \Delta_0^\alpha) \end{cases} \tag{13}$$

with

$$\begin{cases} s^\alpha = K_0^\alpha \sigma^\alpha + K_1^\alpha e_1^\alpha + e_2^\alpha \\ \dot{\sigma}^\alpha = -K_0^\alpha \sigma^\alpha + \mu^\alpha sat(s^\alpha/\mu^\alpha) \end{cases} \tag{14}$$

where μ^α, K_1^α are positive constants. Π_0^α and K_0^α are positive constant.

The controller can be shown to assure the stability of angle of attack and its derivative. For the sake of brevity we skip the proof, that is straightforward and based on a Lyapunov function. It can be shown to go to a residual set that can be attenuated by higher gain. The conclusions we can have are that all errors will be ultimately bounded, where the remaining signals stands for the disturbance on the aircraft speed. It is interesting to remark that variable θ was left free, in order to allow situations as a looping, where θ is continuously varying. Its derivative on the other hand is bounded, and also goes to a residual set (by equation 12).

Since the airspeed control is only a secondary objective, we design a simple PI controller for the thrust to regulate airspeed. Its form is:

$$T = -k_P(V - V_r) - k_I(\dot{V} - \dot{V}_r)$$

where V_r is the airspeed reference, $k_P = 711$ and $k_I = 6.3$.

C. Lateral control design

As in the case of longitudinal control design, in the lateral case it is considered that only lateral state variables are time varying.

$$\begin{cases} \dot{\beta} = \frac{1}{mV}(-\cos(\alpha_0)\sin(\beta)(T + C_x(\alpha_0)\bar{q}S) \\ \quad + \cos(\beta)C_y(\beta)\bar{q}S - \sin(\alpha_0)\sin(\beta)C_z(\alpha_0, \beta)\bar{q}S) \\ \quad + \sin(\alpha_0)p - \cos(\alpha_0)r + \frac{\rho S}{4m}(\cos(\beta)C_{y_p}(\alpha_0)\bar{b}p \\ \quad + \cos(\beta)C_{y_r}(\alpha_0)\bar{b}r) + \frac{g}{V}(\cos(\alpha_0)\sin(\beta)\sin(\theta_0) \\ \quad + \cos(\beta)\cos(\theta_0)\sin(\phi) - \sin(\alpha_0)\sin(\beta)\cos(\phi)) \\ \dot{\phi} = p + \cos(\phi)\tan(\theta_0)r \\ \dot{p} = I_3 C_l(\alpha_0, \beta)\bar{q}S\bar{b} + I_4 C_n(\alpha_0, \beta)\bar{q}S\bar{b} + \frac{\rho V S\bar{b}}{4}[(I_3 C_{l_p}(\alpha_0) \\ \quad + I_4 C_{n_p}(\alpha_0))p + (I_3 C_{l_r}(\alpha_0) + I_4 C_{n_r}(\alpha_0))r] \\ \quad + \bar{q}S[(I_3 C_{l_{\delta_a}}(\alpha_0) + I_4 C_{n_{\delta_a}}(\alpha_0))\delta_a + (I_3 C_{l_{\delta_r}}(\alpha_0) \\ \quad + I_4 C_{n_{\delta_r}}(\alpha_0))\delta_r] \\ \dot{r} = I_4 C_l(\alpha_0, \beta)\bar{q}S\bar{b} + I_9 C_n(\alpha_0, \beta)\bar{q}S\bar{b} + \frac{\rho V S\bar{b}}{4}[(I_4 C_{l_p}(\alpha_0) \\ \quad + I_9 C_{n_p}(\alpha_0))p + (I_4 C_{l_r}(\alpha_0) + I_9 C_{n_r}(\alpha_0))r] \\ \quad + \bar{q}S[(I_4 C_{l_{\delta_a}}(\alpha_0) + I_9 C_{n_{\delta_a}}(\alpha_0))\delta_a + (I_4 C_{l_{\delta_r}}(\alpha_0) \\ \quad + I_9 C_{n_{\delta_r}}(\alpha_0))\delta_r] \end{cases} \tag{15}$$

in which $\bar{b}$ is equivalent length, $I_3 = \frac{I_{zz}}{(I_{xx}I_{zz} - I_{xz}^2)}$, $I_4 = \frac{I_{xz}}{(I_{xx}I_{zz} - I_{xz}^2)}$, $I_9 = \frac{I_{xx}}{(I_{xx}I_{zz} - I_{xz}^2)}$. $C_y(\alpha, \delta_e)$, $C_{y_p}(\alpha_0)$, $C_{y_r}(\alpha_0)$, $C_l(\alpha_0, \beta)$, $C_n(\alpha_0, \beta)$, $C_{l_p}(\alpha_0)$, $C_{n_p}(\alpha_0)$, $C_{l_r}(\alpha_0)$, $C_{n_r}(\alpha_0)$, $C_{l_{\delta_a}}(\alpha_0)$, $C_{n_{\delta_a}}(\alpha_0)$, $C_{l_{\delta_r}}(\alpha_0)$, $C_{n_{\delta_r}}(\alpha_0)$ are lateral aerodynamic coefficients taken from [9].

Aerodynamic force F_y and moments L, N are calculated by their aerodynamic coefficients (see more in [6]). $F_y = (C_y(\beta) + (C_{y_p}(\alpha)p + + C_{y_r}(\alpha)r)\bar{b}/(2V))\bar{q}S$, $L = (C_l(\beta) + C_{l_p}(\alpha, \beta)p\bar{b}/(2V) + C_{l_r}(\alpha, \beta)r\bar{b}/(2V) + C_{l_{\delta_a}}(\alpha)\delta_a + C_{l_{\delta_r}}(\alpha)\delta_r)\bar{q}S\bar{b}$, $N = (C_n(\beta) + C_{n_p}(\alpha, \beta)p\bar{b}/(2V) + C_{n_r}(\alpha, \beta)r\bar{b}/(2V) + C_{n_{\delta_a}}(\alpha)\delta_a + C_{n_{\delta_r}}(\alpha)\delta_r)\bar{q}S\bar{b}$. By replacing F_y, moments L, N and $\alpha = \alpha_0$, $\theta = \theta_0$ in (1). The lateral nonlinear dynamic model used for the control design procedure is consequently reduced as (15).

Equation (15) can be rearranged as:

$$\begin{cases} \begin{bmatrix} \dot{\beta} \\ \dot{\phi} \end{bmatrix} = f_{11}^\beta(\beta, \phi) + f_{12}^\beta(\beta, \phi) \begin{bmatrix} p \\ r \end{bmatrix} \\ \begin{bmatrix} \dot{p} \\ \dot{r} \end{bmatrix} = f_{21}^\beta(\beta, \phi) + f_{22}^\beta(\beta, \phi) \begin{bmatrix} p \\ r \end{bmatrix} + g_2^\beta(\beta, \phi) \begin{bmatrix} \delta_a \\ \delta_r \end{bmatrix} \end{cases} \tag{16}$$

where $f_{11}^\beta(\cdot)$, $f_{12}^\beta(\cdot)$, $f_{13}^\beta(\cdot)$, $f_{21}^\beta(\cdot)$, $f_{22}^\beta(\cdot)$, and $g_2^\beta(\cdot)$ represent the terms of (15) respectively. Equation (16) is mainly used for controller design and stability analysis.

Let us define $x_1^\beta = [\beta, \phi]^T$, $x_2^\beta = \dot{x}_1^\beta = [\dot{\beta}, \dot{\phi}]^T$ and $u^\beta = (\delta_a, \delta_r)^T$, that allow us to rewrite equation (16) to:

$$\begin{cases} \dot{x}_1^\beta &= x_2^\beta \\ \dot{x}_2^\beta &= F^{\beta'}(x_1^\beta, x_2^\beta) + G^{\beta'}(x_1^\beta, x_2^\beta)u^\beta \end{cases} \tag{17}$$

where

$$\begin{cases} F^{\beta'}(\cdot) = (\frac{\partial f_{11}^\beta(\cdot)}{\partial x_1^\beta} + (f^\beta(\cdot) + f_{12}^\beta(\cdot)f_{22}^\beta(\cdot))(f_{12}^\beta(\cdot))^{-1})x_2^\beta \\ -(f^\beta(\cdot) + f_{12}^\beta(\cdot)f_{22}^\beta(\cdot))(f_{12}^\beta(\cdot))^{-1}f_{11}^\beta(\cdot) + f_{12}^\beta(\cdot)f_{21}^\beta(\cdot) \\ G^{\beta'}(\cdot) = f_{12}^\beta(\cdot)g_2^\beta(\cdot) \\ f^\beta(\cdot)\,[p, r]^T = \frac{\partial(f_{12}^\beta(\cdot)[p,r]^T)}{\partial x_1^\beta} \end{cases} \tag{18}$$

We define an output error vector $e_1^\beta = x_1^\beta - x_{1ref}^\beta$ and $e_2^\beta = \dot{e}_1^\beta$ where $x_{1ref}^\beta = (\beta_{ref}, \phi_{ref})^T$ is the output reference considered as constant. Equation (18) can be transformed into (12) with two new state variables e_1^β and e_2^β.

$$\begin{cases} \dot{e}_1^\beta &= e_2^\beta \\ \dot{e}_2^\beta &= F^\beta(e_1^\beta, e_2^\beta) + G^\beta(e_1^\beta, e_2^\beta)u^\beta \end{cases} \tag{19}$$

$G^\beta(x_1^\beta, x_2^\beta)$ is invertible, and $F^\beta(x_1^\beta, x_2^\beta)$ and $G^\beta(x_1^\beta, x_2^\beta)$ are Lipschitz in the considered domain of $x_1^\beta = [\beta, \phi]^T$, $\dot{x}_1^\beta = x_2^\beta$ with $\beta \in (-30°, 30°)$ and $\phi \in (-90°, 90°)$.

Application of control law (7) for system (19) leads to the controller:

$$\begin{cases} u^\beta = -\Pi^\beta(\cdot)\text{sat}(s^\beta/\mu^\beta) \\ \Pi^\beta(\cdot) = (G^\beta)^{-1}(\cdot)(\Pi_0^\beta + \mu^\beta K_0^\beta + (\gamma^\beta(\cdot) + \Delta_0^\beta)I_2) \end{cases} \tag{20}$$

with

$$\begin{cases} s^\beta = K_0^\beta \sigma^\beta + K_1^\beta e_1^\beta + e_2^\beta \\ \dot{\sigma}^\beta = -K_0^\beta \sigma^\beta + \mu^\beta sat(s^\beta/\mu^\beta) \end{cases} \tag{21}$$

where $\lambda^\beta = min(\|G^\beta(\cdot)\|)$ for $\beta \in (-30°, 30°)$, $\phi \in (-180°, 180°)$. Π_0^β is a constant large enough, μ^β is the boundary layer, K_0^β and K_1^β are positive definite matrices chosen such a way that $K + sI_2$ is Hurwitz.

IV. Simulation Results

In section III, the design methodology of the conditional servo-compensator controller to stabilize the angle of attack, sideslip and roll angle is proposed when full knowledge of the aerodynamic characteristics is available. This section presents numerical simulation results for the controller to demonstrate the performance of the proposed conditional servo-compensator control laws in the drop phase.

As mentioned in section II, we have considered the launch phase as disturbances on aerodynamic force and moments during a time interval T_{int}, and that the model following the launch phase is that of an F-16. This model is used since it has already been applied for (manned) airlaunch, and because its nonlinear model, wind tunnel informations and data are widely known and used for control design. It is important to remark that the model used in the following simulations is even more complete than that used in the control design, for example it includes actuator dynamics and their limitations. As a consequence, simulations also illustrate some properties of robustness to unmodeled dynamics.

In the following simulations, we have simultaneously applied the SISO longitudinal controller for angle of attack, and the MIMO lateral one for the sideslip and roll angles in the full nonlinear F-16 aircraft model. We may note that the control inputs are limited by their physical characteristics introduced in section II.

The control law in (7) whose $\Pi(\cdot)$ can be written a simplier way as:

$$\Pi(\cdot) = (G^i)^{-1}(\Pi_0 + \gamma(\cdot)I_n) \tag{22}$$

in which, $\gamma(\cdot) = \gamma_1\|e_1\|^2 + \gamma_2\|e_2\|^2$, γ_1 and γ_2 are positive constant. n = 1 for the longitudinal case and n = 2 for the lateral case.

Application of this control law to two motion modes presented in subsections (III-B) and (III-C) is done by determining the set of parameters Π_0^i, γ_1^i, γ_2^i, μ^i, K_1^i and K_0^i with $i = \alpha, \beta$ corresponding to longitudinal mode and lateral mode respectively.

Π_0^α	μ^α	γ_1^α and γ_2^α	k_0^α	K_1^α
25.0	1.0	0.001 and 0.001	1.1	1.8
Π_0^β	μ^β	γ_1^β and γ_2^β	K_0^β	K_1^β
$\begin{bmatrix}4.00.0\\0.05.0\end{bmatrix}$	1.0	0.001 and 0.001	$\begin{bmatrix}0.80.0\\0.01.1\end{bmatrix}$	$\begin{bmatrix}1.50.0\\0.01.8\end{bmatrix}$

TABLE I
PARAMETERS FOR TWO CONTROLLERS

We will stabilize the second model following the launch phase to its equilibrium point $(V, h) = (154m/s, 5000m)$ corresponding to (angle of attack α_r to 4.6°, sideslip β_r to 0°, and roll angle ϕ_r to 0°).

Its initial condition is the final state of the first model ($\alpha = 10.6°$, $\beta = 0°$ and $\phi = 0°$) as in Section II. Moreover, we add on its initial condition a small disturbance on system output. That means the initial condition of second model is ($\alpha_0 = 17.5°$, $\beta_0 = 4°$ and $\phi_0 = 15°$) for all numerical simulations.

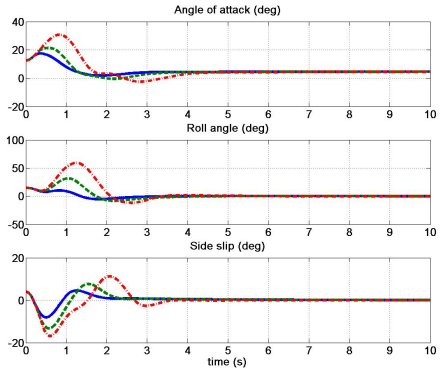

Fig. 2. Angle of attack, Sideslip Angle and Roll angle stabilized

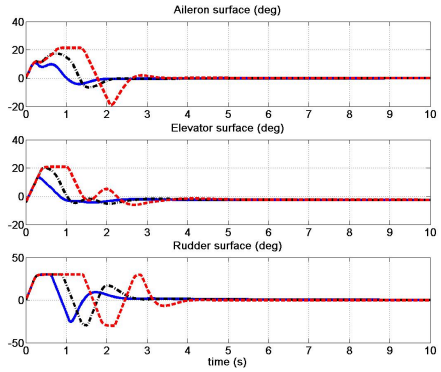

Fig. 3. Aileron, Elevator and Rudder

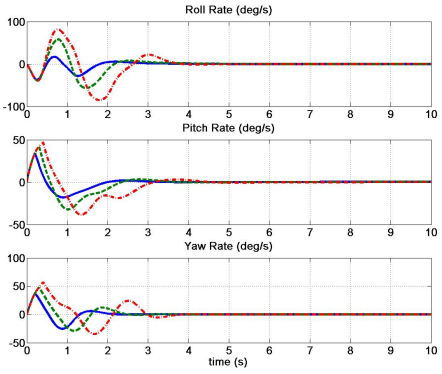

Fig. 4. State variables: Angular rates of system

The second model is disturbed on its aerodynamic force and moments during an interval T_{int} as in Section II. We simulate three sets of time lengths:

1) $T_{int} = 0.2s$ (corresponding to solid lines in Fig. 2 to Fig. 5) produces damped oscillations (see in [11]).
2) $T_{int} = 0.3s$, (the dashed lines in Fig. 2 to Fig. 4), it was shown in [11] that the system controlled by a LQR controller becomes completely unstable for this length.
3) $T_{int} = 0.4s$ (corresponding to dash dotted lines in Fig. 2 to Fig. 5) one can see that the controller is still able to stabilize the system.

Fig. 2 illustrates the convergence of the system output to the operating point of the aircraft at the end of 5s without static steady error for the three cases of $T_{int} = (0.2s, 0.3s, 0.4s)$. All system outputs are still under their physical limitation.

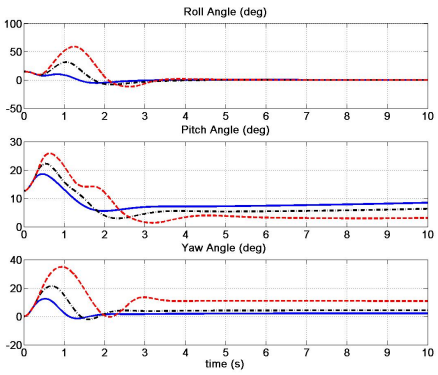

Fig. 5. State variables: Euler's angles of system

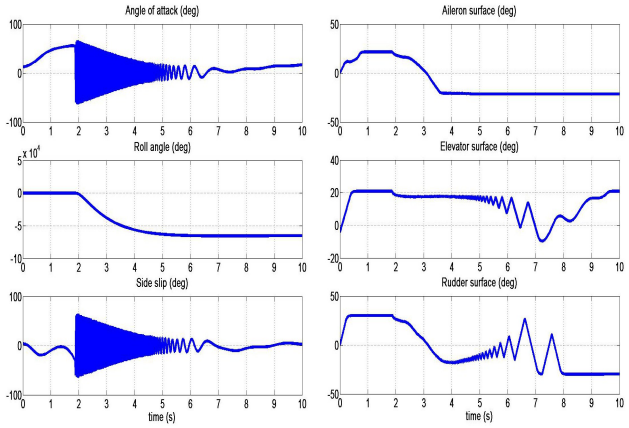

Fig. 6. System's output unstable and Control surfaces

Figs. 4 shows that angular rates converge to zero in all cases and Fig. 5 the convergence of Euler's angles.

In Fig. 3, it can be seen that the control variables are saturated by their physical limitations due to a high perturbation on aerodynamic forces and moments.

For $T_{int} = (0.2s, 0.3s)$ the system is well stabilized, while for T_{int} assuming larger values the system becomes more oscillatory and attains its limits of stability, the case of $T_{int} = 0.4s$ is an example. We show in Fig. 6 that the system will be unstable even with the robust conditional servo-compensator controller for an interval $T_{int} = 0.49s$.

V. Conclusion

This work has studied the airlaunch system at the stage separation from the reusable airlaunch vehicle from the down stage and the effects of the stage separation phase in the stability of the airlaunch system. The separation phase may produces large impulses on forces and moments, making the system unstable. These impulses are considered to last a time interval, that is then evaluated in simulations.

To stabilize the airlaunch system after this stage separation phase, a conditional servo-compensator control is considered. This controller is designed using an F-16 model representing the aircraft just after dropping the second stage, but disturbed by large impulses. For a perturbation on aerodynamic forces and moments during an interval T_{int}, the stability of the system after the drop stage may be assured for small time intervals. When T_{int} becomes large, the system becomes unstable even with the proposed controller.

In future works other disturbances can be considered, as well as other control strategies for this particularly interesting and difficult problem.

References

[1] Gilney Damm and Van Cuong Nguyen. Mimo conditional servo-compensator control for a class of nonlinear systems (accepted). *In Proceedings of the 51th Conference on Decision and Control, Maui - Hawaii, USA.*, December 10-13, 2012.

[2] Gilney Damm and Van Cuong Nguyen. Mimo conditional integrator control for a class of nonlinear systems. In *In proceedings of System Theory, Control, and Computing (ICSTCC), 2011 15th International Conference, Sinaia, Romania*, October 14-16, 2011.

[3] Gary C. Hudson. Quickreach responsive launch system. In *4th Responsive Space Conference, Los Angeles, CA, USA*, April 24-27, 2006.

[4] Hassan K. Khalil. On the design of robust servomechanisms for minimum phase nonlinear systems. *Robust Nonlinear Control 2000, John Wiley & Sons*, 10:339–361, 2000.

[5] Hassan K. Khalil. *Nonlinear Systems*. Prentice Hall, 2001.

[6] Taeyoung Lee and Youdan Kim. Nonlinear adaptive flight control using backstepping and neural networks controller. *Journal of guidance, control and dynamics*, 24:675–682, 2001.

[7] Nazmi A. Mahmoud and Hassan K. Khalil. Robust control for a nonlinear servomechanism problem. *International Journal of Control*, 66:779–802, April 1, 1997.

[8] Attaullah Y. Memona and Hassan K. Khalil. Output regulation of nonlinear systems using conditional servocompensators. *Automatica*, 46:1119–1128, July, 2010.

[9] Eugene Morelli. Global nonlinear parametric modeling with application to f-16 aerodynamics. *In Proceedings of the 1998 American Control Conference, Philadelphia, PA , USA*, 2:997–1001, Junuary 21-26, 1998.

[10] L.T. Nguyen, M.E. Ogburn, and P. Deal. Simulator study of fighter airplane with relaxed longitudinal static stability. *Technical report NASA*, page 1538, 1979.

[11] Van Cuong Nguyen and Gilney Damm. Modeling and conditional integrator control of an unmanned aerial vehicle for airlaunch. *in Proceedings of the 2012 American Control Conference (ACC), Montreal, Canada*, June 27-29, 2012.

[12] Van Cuong Nguyen and Gilney Damm. Mimo conditional integrator control for unmanned airlaunch. In *In proceedings of System Theory, Control, and Computing (ICSTCC), 2011 15th International Conference, Sinaia, Romania*, October 14-16, 2011.

[13] Jan Roskam. *Airplane Flight Dynamic and Automatic Flight Controls, Part 1*. Design, Analysis and Research Corporation, 2001.

[14] Marti Sarigul-Klijn and Nesrin Sarigul-Klijn. Selection of a carrier aircraft and a launch method for air launching space vehicles. In *AIAA SPACE 2008 Conference and Exposition, San Diego, California, USA*, September 9 - 11, 2008.

[15] Sridhar Seshagiri and Hassan K. Khalil. Robust output feedback regulation of minimum-phase nonlinear systems using conditional integrators. *Automatica*, 41:43–54, January, 2005.

[16] Lars Sonneveldt. *Nonlinear F-16 Model Description*. Delft University of Technology, Netherlands, 2006.

[17] Peter H. Zipfel. *Modeling and Simulation of Aerospace Vehicle Dynamics, 2nd edition*. American Institute of Aeronautics and Astronautics, January, 2001.